Organic & Biomolecular Chemistry

ROYAL SOCIETY OF CHEMISTRY

PAPER

View Article Online
View Journal | View Issue

Cite this: *Org. Biomol. Chem.*, 2020, **18**, 4590

Balancing interactions in proline-based receptors for chiral recognition of L-/D-DOPA†

Lin-E. Guo, Yu-Xin Tang, Shu-Ying Zhang, Yuan Hong, Xiao-Sheng Yan, Zhao Li and Yun-Bao Jiang *

Received 7th March 2020,
Accepted 28th May 2020

DOI: 10.1039/d0ob00493f

rsc.li/obc

Proline based receptors (**1–14**) attached with phenylboronic acid and benzaldehyde binding groups at the N-/C- or C-/N-termini of the proline residue were created for chiral recognition of L-/D-DOPA, in an attempt to examine if balancing the two binding events would influence the recognition. By changing the positions of boronic acid and aldehyde groups substituted on the phenyl rings (**1–4**, **5–8**) and the site at which phenylboronic acid and benzaldehyde moieties attached respectively to the N- and C-termini or C- and N-termini of the proline residue (**1–4** *vs.* **5–8**), and by introducing an electron-withdrawing fluorine atom in the phenyl ring of the weaker binder the benzaldehyde moiety (**11** *vs.* **1**, **14** *vs.* **5**), we were able to show that a better balance of the two binding events does improve the chiral recognition. This finding can only be made with the current version of receptors that were equipped with two different binding groups. Together with the finding that the chiral recognition performance in mixed organic–aqueous solutions is tunable by varying the solvent composition, we have now arrived at a protocol for designing proline based receptors for extended applications in chiral recognition.

Introduction

Proline is a naturally occurring, structurally rigid amino acid and thereby plays an essential role in maintaining the secondary structures of peptides/proteins, such as β-turns,[1] allowing the construction of peptidomimetics for drug discovery.[2] The rigid and folded structural character of this chiral amino acid has also been employed for other applications, for example to develop asymmetric organocatalysts.[3] We were thus inspired to initiate our efforts to develop cleft-shaped proline-based receptors, for chiral recognition, as both their N- and C-termini can be readily equipped with different binding groups, depending on the species to be recognized. Recently we reported our first example for the chiral recognition of glucose.[4] In that protocol, proline was derived with two phenylboronic acid groups at the N- and C-termini to allow for an efficient chiral recognition of glucose. The positions of the boronic acid groups in the phenylboronic acid moieties can be varied to optimize the recognition performance; the two phenylboronic acid groups are however more or less the same in terms of the affinity towards the *cis*-1,2- or 1,3-diol units in the glucose molecule. Differences in the recognition ability thus result mainly from the steric factor of the two binding groups. The contribution of the difference in the binding abilities of the two binding groups that can at least be incorporated into the proline residue remains to be identified, so does the contribution of the intrinsic character of the proline residue, *i.e.* the ratio of its *trans*- to *cis*-conformers. We therefore extended our efforts towards proline-based receptors containing two different binding groups. For this purpose, we chose to design receptors for the chiral recognition of L- and D-DOPA (Scheme 1) *via* interactions with its *cis*-diol and amine groups. We created a series of proline derivatives bearing boronic acid and aldehyde binding groups in the forms of phenylboronic acid and benzaldehyde, respectively, which are placed at the N- and C-termini of the proline residue (Scheme 1). We further attempted to fine tune the binding by introducing electron-withdrawing fluorine atoms in the phenylboronic acid and/or benzaldehyde groups and by varying the ratio of *cis*- to *trans*-conformers of the proline residue in MeOH/aqueous buffer solutions.

3,4-Dihydroxy-L-phenylalanine (L-DOPA) is the precursor of the neurotransmitter dopamine and an important agent for Parkinson's disease, whereas its D-enantiomer displays neurotoxic side effects.[5] This is another reason we chose the chiral recognition of L-/D-DOPA to examine the performance of our new receptors. As a catecholamine derivative, DOPA has been detected mainly by liquid chromatography, thin-layer chromatography, capillary electrophoresis, mass spectrometry and electrochemical methods,[6] while chiral recognition of DOPA

Department of Chemistry, College of Chemistry and Chemical Engineering, The MOE Key Laboratory of Spectrochemical Analysis and Instrumentation, and iChEM, Xiamen University, Xiamen 361005, China. E-mail: ybjiang@xmu.edu.cn

†Electronic supplementary information (ESI) available: Experimental details, additional figures, and characterization data. See DOI: 10.1039/d0ob00493f

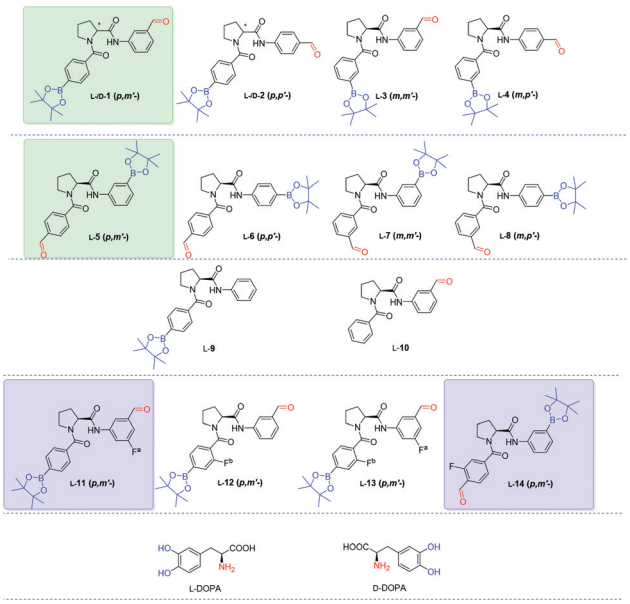

Scheme 1 Chemical structures of receptors L-/D-**1** (*p*,*m*′-), L-/D-**2** (*p*,*p*′-), L-**3** (*m*,*m*′-) and L-**4** (*m*,*p*′-), receptors L-**5** (*p*,*m*′-), L-**6** (*p*,*p*′-), L-**7** (*m*,*m*′-) and L-**8** (*m*,*p*′-), and chiral compounds L-/D-DOPA. L-**9** and L-**10** are control compounds of L-**1**. Compounds L-**11**, L-**12** and L-**13** are fluorine-substituted derivatives of L-**1**; L-**14** is a fluorine-substituted derivative of L-**5**. "*" on the structures highlights the chiral carbon.

has been realized *via* its interaction with fluorescent probes, surface-functionalized electrodes, and chiral polymers.[7] Receptors for DOPA chiral recognition could contain a boronic acid and an aldehyde group to form a five-membered cyclic boronate and imine with DOPA.[7a,8] Boronic acid and aldehyde groups were therefore introduced into the proline residue, employing the boronic acid/*cis*-diol interaction and imine formation reaction, respectively.[8] With these designed receptors we identified the contribution of the balanced affinities of the binding groups in tuning the chiral recognition performance of the receptors. Circular dichroism (CD) spectroscopy, as a powerful technique for chiral research,[9] is the major method we employed in this work to evaluate the chiral recognition performance.

Results and discussion

Design and characterization of receptors

L-/D-**1**, L-/D-**2**, and L-**3** to L-**14** (Scheme 1) were designed and synthesized. Receptors **1–8** differ in the positions of boronic acid and aldehyde binding groups substituted, respectively, on the two phenyl rings (**1–4** and **5–8**) or the site of the phenylboronic acid and benzaldehyde moieties attached at the N- and C-termini of the proline residue (**1–4** *vs.* **5–8**), while **9** and **10** containing only the phenylboronic acid or benzaldehyde moiety, respectively, are the control compounds of **1**. **11–14** are fluorinated **1** or **5**, **11–13** *vs.* **1**, and **14** *vs.* **5** (Scheme 1).

Their absorption and CD spectra were studied in the optimized media referring to binding, 7 : 3 (v/v) MeOH/0.05 M, pH 8.0 PBS buffer (Fig. S1, ESI†). Receptors L-**1** to L-**4**, with a phenylboronic acid moiety at the N-terminal while a benzaldehyde moiety at the C-terminal, exhibit a major absorption at 238 nm (**1** and **3**) or 299 nm (**2** and **4**) (Fig. S2, ESI†). L-**5** to L-**8**, in which the phenylboronic acid moiety locates at the C-terminal while the benzaldehyde moiety is at the N-terminal, exhibit absorptions at 245 nm and 250 nm, respectively (Fig. S2, ESI†). CD signals of L-**1** to L-**4** appear at 238 nm or 292 nm, while those of L-**5** to L-**8** at 245 nm and 260 nm (Fig. S3, ESI†), both of which suggest that the chirality of the proline residue has transferred to the achiral phenylboronic acid and benzaldehyde chromophores. This chirality transfer was found to occur in L-**9** to L-**14** too, as observed from their absorption and CD spectra (Fig. S4 and S5, ESI†).

As a structural character of the proline residue,[10,14] receptors **1–14** showed both *cis*- and *trans*-conformers and in 7 : 3 (v/v) MeOH/0.05 M pH 8.0 PBS buffer solution the ratios of *cis*- to *trans*-conformers, deduced from ^{1}H NMR spectra, are all around 0.5 (Table 1). DFT calculations indicate that L-**1** favors the *trans*-form over the *cis*-form by 9.04 kJ mol^{-1}, and by 9.32 kJ mol^{-1} for L-**11** (Fig. 1).

Positions of boronic acid and aldehyde groups on phenyl rings

The absorption and CD spectra of L-**1** to L-**8** in the presence of L- and/or D-DOPA were monitored to evaluate DOPA sensing efficiency (Fig. 2 and 3). L-**1** exhibits a substantial CD response toward D-DOPA (Fig. 2a) making the CD signal at 250 nm change drastically, while a new signal appears at 303 nm, accompanied by an isosbestic wavelength of 290 nm. This means that L-**1** and D-DOPA form a structurally well-defined complex. Indeed, a Job plot indicates a 1 : 1 stoichiometry between L-**1** and D-DOPA (Fig. S6, ESI†). However, L-DOPA only triggers an enhanced CD signal at 255 nm (Fig. 2b), indicating thereby a considerable chiral recognition performance of L-**1** for D- over L-DOPA (K_a^D = 1.72 × 10^5 M^{-1}, K_a^L = 6.44 × 10^4 M^{-1} and K_a^D/K_a^L = 2.67, Table 1). L-**1**, among L-**1** to L-**4**, shows the best chiral recognition toward D-DOPA, while L-**2** and L-**3** prefer to bind to L-DOPA and L-**4** shows a negligible CD response toward L- and D-DOPA (Table 1 and Fig. 2). Likewise, D-**1** shows a significant CD response toward L-DOPA, suggesting the role that the steric matching in L-**1**/D-DOPA and in D-**1**/L-DOPA (Fig. S7, ESI†) plays, as mirror-imaged CD profiles for L-**1**/D-DOPA and D-**1**/L-DOPA were observed (Fig. S8, ESI†). It is thus shown that boronic acid and aldehyde groups substituted at significant positions of the two phenyl rings do matter in the chiral recognition,[4] and the *para*-/*meta*-substitution combination (**1**) exhibits the best performance (Table 1).

L-**9** and L-**10** containing only the phenylboronic acid or benzaldehyde moiety, control compounds of L-**1**, show negligible CD responses toward L-/D-DOPA (Fig. S9 and S10, ESI†). This means that L-**1** binds to D-DOPA using both its boronic acid and aldehyde groups, to form likely a rigid complex,[4] in which an efficient chirality transfer occurs.

Table 1 Binding constants (K_a) of L-**1** to L-**8**, and L-**11** to L-**14** with L-/D-DOPA and the ratio of binding constants with D- to L-DOPA (K_a^D/K_a^L)[a]

Receptor	Ratio (*cis*-/*trans*-conformers)	K_a/M^{-1} L-DOPA	K_a/M^{-1} D-DOPA	K_a^D/K_a^L
L-**1**	0.49	$(6.44 \pm 0.99) \times 10^4$	$(1.72 \pm 0.18) \times 10^5$	2.67
D-**1**	0.47	$(1.27 \pm 0.15) \times 10^5$	$(5.35 \pm 0.96) \times 10^4$	0.42[b]
L-**2**	0.47	$(1.97 \pm 0.19) \times 10^4$	—[c]	—
D-**2**	0.46	—[c]	$(1.60 \pm 0.25) \times 10^4$	—
L-**3**	0.54	$(3.22 \pm 0.62) \times 10^4$	$(2.60 \pm 0.61) \times 10^4$	0.81
L-**4**	0.45	—[c]	—[c]	—
L-**5**	0.50	$(6.04 \pm 1.14) \times 10^4$	$(3.15 \pm 0.66) \times 10^4$	0.52[d]
L-**6**	0.46	—[c]	—[c]	—
L-**7**	0.47	$(7.38 \pm 1.15) \times 10^4$	$(5.42 \pm 1.52) \times 10^4$	0.73
L-**8**	0.44	—[c]	—[c]	—
L-**11**	0.33	$(1.13 \pm 0.15) \times 10^5$	$(1.36 \pm 0.89) \times 10^6$	12.0
	0.33[e]	1.35×10^5 [e]	1.57×10^6 [e]	11.6[e]
L-**12**	0.47	$(1.07 \pm 0.23) \times 10^5$	$(1.91 \pm 0.49) \times 10^5$	1.79
L-**13**	0.55	$(1.13 \pm 0.25) \times 10^5$	$(1.82 \pm 0.51) \times 10^5$	1.61
L-**14**	0.52	$(1.12 \pm 0.40) \times 10^6$	$(8.23 \pm 2.51) \times 10^4$	0.07[f]

[a] Binding constants (K_a), if not otherwise indicated, were obtained by nonlinear fitting of the CD signal as a function of DOPA concentration assuming a 1 : 1 stoichiometry (Fig. S35–S39, ESI†). [L-**1**] to [L-**8**] = 40 μM, [L-**11**] = 50 μM, [L-**12**] = 60 μM, [L-**13**] = 50 μM, [L-**14**] = 50 μM, T = 298 K. [b] The corresponding ratio of binding constants with L- to D-DOPA, K_a^L/K_a^D, is 2.37. [c] Due to minor changes in CD spectra, accurate K_a values could not be fitted (titration curves in Fig. S40–S59, ESI†). [d] The corresponding K_a^L/K_a^D is 1.92. [e] Obtained by ^{19}F NMR titrations. [f] K_a^L/K_a^D is 13.6.

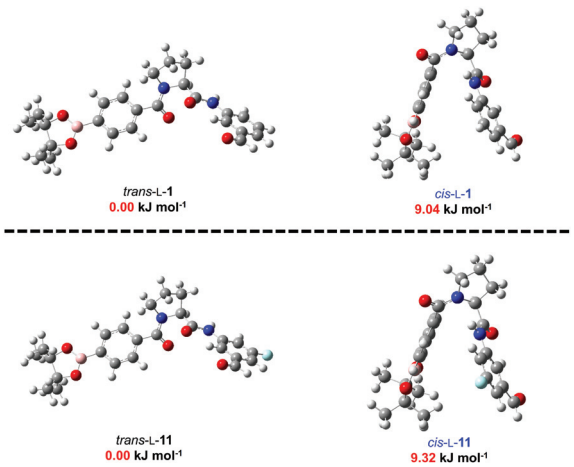

Fig. 1 DFT-optimized structures of *trans*-/*cis*-L-**1** and *trans*-/*cis*-L-**11** in H_2O at the B3LYP/6-31G* level. Energies are given in relative values.

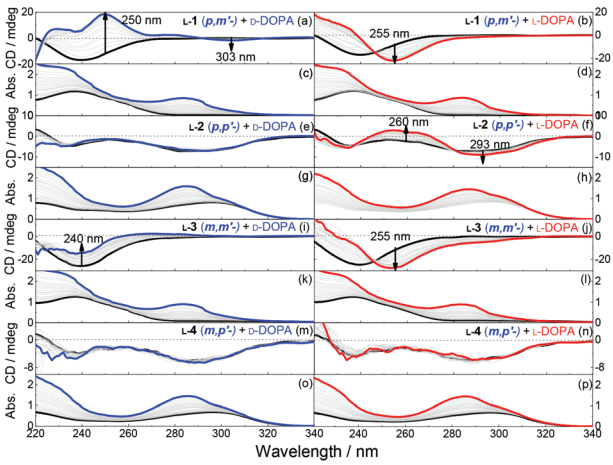

Fig. 2 Evolution of absorption and CD spectra of L-**1** (*p*,*m*′-), L-**2** (*p*,*p*′-), L-**3** (*m*,*m*′-) and L-**4** (*m*,*p*′-) upon mixing with D-DOPA or L-DOPA in 7 : 3 (v/v) MeOH/0.05 M, pH 8.0 PBS buffer. [L-**1**] = [L-**2**] = [L-**3**] = [L-**4**] = 40 μM, [D-DOPA] = [L-DOPA] = 0–250 μM.

Sites of phenylboronic acid and benzaldehyde moieties at the N-/C-termini of the proline residue

Receptors L-**5** to L-**8** differ from L-**1** to L-**4** in the sites of phenylboronic acid and benzaldehyde moieties that are attached to the proline residue, at the N- or C-terminal (Scheme 1). The available binding constants indicate that L-**5** to L-**8** prefer to bind to L-DOPA and **5**, again in the *para*-/*meta*-substitution profile, among **5**–**8**, showing the best recognition, *e.g.* for L-DOPA in the case of L-**5**, an observation similarly made in the series of **1**–**4** (Table 1). Yet the chiral recognition ability of L-**5** for L-DOPA is lower than that of L-**1** toward D-DOPA (Table 1). The site where the two moieties containing binding groups are attached in the proline residue (**1**–**4** *vs.* **5**–**8**) is therefore shown to influence their binding preference towards D- or L-DOPA, despite not much effect on the binding constant. This observation can only be made by using the current version of proline-based receptors that are equipped with two *different* binding groups that are expected to bind simultaneously with DOPA.

Fluorine substitution for enhancing chiral recognition

Data presented in Table 1 suggest that the chiral recognition of L-**1** to L-**8** could still be improved. A possible way forward is to enhance the relatively weaker interaction of the aldehyde in the receptor molecule with the amine in DOPA, compared to that between boronic acid in the receptor and *cis*-diol in

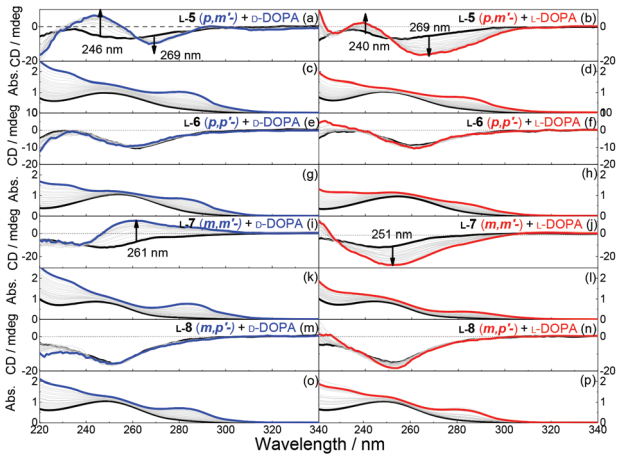

Fig. 3 Evolution of the absorption and CD spectra of L-**5** (*p*,*m*′-), L-**6** (*p*,*p*′-), L-**7** (*m*,*m*′-) and L-**8** (*m*,*p*′-) upon mixing with D-DOPA and L-DOPA in 7 : 3 (v/v) MeOH/0.05 M, pH 8.0 PBS buffer. [L-**5**] = [L-**6**] = [L-**7**] = [L-**8**] = 40 μM, [D-DOPA] = [L-DOPA] = 0–250 μM.

DOPA. Substitution of an electron-withdrawing group on the phenyl ring, which is expected to increase the reactivity of the aldehyde toward the amine and boronic acid toward *cis*-diol, is a choice for fine tuning of the binding balance of the two binding groups. In such a way the binding and chiral recognition as well might be enhanced if the binding to the aldehyde moiety is promoted, for example by introducing an electron-withdrawing fluorine atom, expected to increase more the electrophilicity of aldehyde C═O and thereby enable faster imine formation.[11] Substitution of fluorine atom(s) was done also because ^{19}F NMR covers a broad chemical shift range with practically no background signal[12] and high sensitivity to subtle structural changes,[13] and ^{19}F NMR could be employed to follow the binding.

Substitution by fluorine on receptor L-**1**, leading to L-**11** to L-**13** (Scheme 1), was carried out. Fig. 4a and Fig. S11a† show that the addition of D-DOPA results in an increasing CD signal of L-**11** at 248 nm, while a new negative signal at 303 nm develops, with an isosbestic point at 290 nm. This observation is similar to that made with L-**1** (Fig. 2a), meaning that a well-defined structure forms between L-**11** and D-DOPA too. The interaction takes place quickly and it reaches equilibrium in 10 minutes (Fig. S12, ESI†). A 1 : 1 stoichiometry between L-**11** and D-DOPA was found in the Job plot (Fig. S13, ESI†). A peak at *m*/*z* 558.1853 ($C_{29}H_{26}BFN_3O_7^-$, [M + OCH_3]$^-$) identified in the mass spectrum (Fig. S14, ESI†) confirms the 1 : 1 binding stoichiometry, whereas, the presence of L-DOPA (Fig. 4b and Fig. S11b, ESI†) only induces a new CD signal at 255 nm, although a 1 : 1 binding was also suggested by the peak at *m*/*z* 534.1685 ($C_{56}H_{45}B_2F_2N_6O_{13}^{2-}$, [2M − 2H]$^{2-}$) (Fig. S15, ESI†). It was concluded that L-**11** and D-DOPA form a 1 : 1 cyclic complex through two-point interactions[4] that lead to boronate and imine, displaying thereby a chiral recognition of D-DOPA over L-DOPA (Fig. 4c). Despite similar profiles in the variations of CD spectra of L-**1** and L-**11** in the presence of D-DOPA (Fig. 2a, 4a and Fig. S16, ESI†), the interaction of L-**11** with D-DOPA is much more dramatic than that of L-**1** (Fig. S16c and d, ESI†). The binding constant of L-**11**/D-DOPA, (1.36 ± 0.89) × 10^6 M^{-1}, is higher by one order of magnitude than that of L-**1**/D-DOPA of (1.72 ± 0.18) × 10^5 M^{-1}. More significantly, the ratio of the binding constants, K_a^D/K_a^L of L-**11** for D-/L-DOPA of 12.0, is also much higher than that of L-**1** (2.67, Table 1). Fluorine substitution at the benzaldehyde moiety indeed greatly enhances the binding and significantly the chiral recognition. When fluorine is substituted at the benzaldehyde moiety of L-**5**, the isomer of L-**1** but with an opposite location of the two binding moieties and a preference to bind to L-DOPA, the resultant receptor L-**14** (Scheme 1) shows a binding constant with L-DOPA of (1.12 ± 0.40) × 10^6 M^{-1} (Table 1 and Fig. S17, ESI†), 18.5 times that of L-**5**/L-DOPA, as well as a much higher K_a^L/K_a^D (13.6 *vs.* 1.92, Table 1). The chiral recognition of L-**14** for L-DOPA is therefore dramatically enhanced, even better than those of some of the reported recognition systems.[7e,8c]

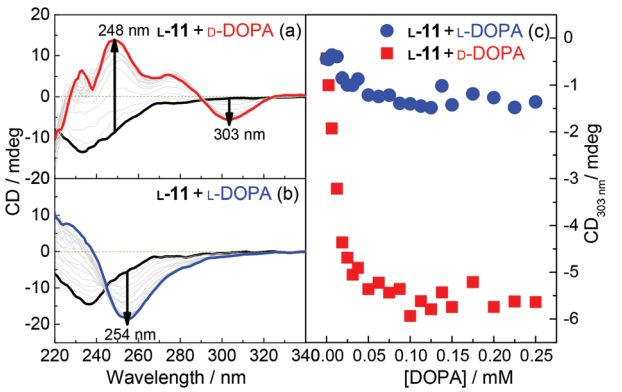

Fig. 4 CD spectra (a and b) and CD intensity at 303 nm (c) of L-**11** in the presence of D- or L-DOPA in 7 : 3 (v/v) MeOH/0.05 M, pH 8.0 PBS buffer. [L-**11**] = 40 μM, [DOPA] = 0–250 μM.

We also examined the chiral recognition of receptors L-**12** and L-**13**, the isomers of L-**11**, in which fluorine atoms are substituted at either the phenylboronic acid phenyl ring or both the phenylboronic acid and benzaldehyde moieties. Spectral response profiles of L-**12** and L-**13** toward L-/D-DOPA (Fig. S18 and S19, ESI†) are similar to those of L-**11**, yet the binding to D-DOPA is much weaker while that to L-DOPA is similar (Table 1). The chiral recognition is weaker, with the K_a^D/K_a^L values of 1.79 and 1.61, respectively, being lower than that of L-**11** (12.0, Table 1). This means that fluorine substitution at the phenylboronic acid moiety (L-**12**), even in the case of L-**13** in which a fluorine atom is also substituted at the benzaldehyde moiety, destroys the benefit of fluorine substitution at benzaldehyde only. It is therefore made clear that the introduction of a fluorine atom only into the phenylaldehyde moiety that leads to enhanced imine formation and therefore a better balance of the two interactions of receptor L-**11** with DOPA, results in a much stronger binding to L-/D-DOPA and a higher recognition of D-DOPA over L-DOPA. The same holds true for L-**14**, a derivative of L-**5** with a fluorine atom substituted on the

benzaldehyde phenyl ring, with a higher chiral recognition of L-DOPA.

^{1}H NMR and ^{19}F NMR titrations were applied to probe the binding of L-**11** with L-/D-DOPA. ^{1}H NMR assays indicate that the *cis*- to *trans*-conformer ratio of L-**11** is 0.33 in 7 : 3 (v/v) CD_3OD/0.05 M PBS, pH 8.0 (PBS dissolved in D_2O) (Fig. S20, ESI†). Upon addition of D-DOPA, the resonances of protons on the aromatic rings (Fig. S21, ESI†) and the proline methylene (Fig. S22, ESI†) become well-resolved, while that of the aldehyde proton disappears (Fig. S23, ESI†). This supports the rigid structure of the formed L-**11**/D-DOPA complex, *via* the two-point interaction mode.[4] However, in the presence of L-DOPA, the resonances of aromatic protons of L-**11** are broadened (Fig. S24 and S25, ESI†), suggesting a large scale structure with flexibility and a weak interaction of L-**11** with L-DOPA, which is directly supported by mass spectral data (Fig. S15, ESI†). The ^{19}F NMR spectra are much simpler that they allow a better evaluation of the chiral recognition. Fig. 5 shows ^{19}F NMR spectra of L-**11** in the presence of D-DOPA and/or L-DOPA. Two sets of ^{19}F NMR signals (−111.7 ppm and −113.4 ppm) are observed for L-**11** (Fig. 5a and Fig. S26, ESI†), assigned to the *trans*- and *cis*-conformers, respectively. In the presence of 0–4 equivalents of D-DOPA, the ^{19}F NMR signal at −111.7 ppm sharply decreased and that at −113.4 ppm disappeared, while a new signal at −112. 3 ppm developed (Fig. 5b and Fig. S26, ESI†). In the presence of L-DOPA, a ^{19}F NMR signal at −113.4 ppm developed (Fig. 5c and Fig. S27, ESI†), while the original signal at −111.7 ppm decreased and that at −113.4 ppm largely remained. ^{19}F NMR competitive experiments were also carried out, by mixing L-**11** (120 μM) with L-DOPA (480 μM) and D-DOPA (480 μM). New signals at −112.3 ppm and −113.4 ppm developed at a ratio of 1.0 : 0.23 (Fig. 5d). This value again shows that L-**11** exhibits a superior chiral recognition toward D-DOPA. ^{19}F NMR titrations also allow the binding constants of L-**11** with D- and L-DOPA to be evaluated as 1.57×10^6 M^{-1} and 1.35×10^5 M^{-1}, respectively, with a K_a^D/K_a^L ratio of 11.6 (Table 1 and Table S1, ESI†), all being consistent with those obtained by CD titrations (Table 1).

Changing the solvent composition for enhancing chiral recognition

The ratio of *cis*- to *trans*-conformers of the proline residue is sensitive to the polarity of the solvent.[14] All the aforementioned experiments were carried out in the same solvent. ^{1}H NMR measurements show that the ratio values of **1–14** are more or less the same in that solvent, around 0.5 (Table 1). The differences in the binding of receptors **1–14** to DOPA therefore are not due to the difference in the conformation distribution of the proline residue. However, our DFT calculations show that, despite both *trans*- and *cis*-conformers of L-**11** binding more strongly with D-DOPA than with L-DOPA, the *cis*-L-**11**/D-DOPA complex is slightly more stable than the *trans*-L-**11**/D-DOPA complex (Fig. 6 and Fig. S28, ESI†). It is therefore assumed that L-**11** in the L-**11**-D-DOPA complex exists in its *cis*-conformation. This is supported by ^{19}F NMR titrations with D-DOPA (Fig. S26, ESI†) that show that the disappearance of the ^{19}F NMR signal of *cis*-L-**11** at −113.4 ppm is faster than that of the *trans*-conformer (Table S2, ESI†). We therefore extended our study to examine if the ratio of the *cis*-/*trans*-conformers of the proline residue in the receptor molecule, if tunable, exerts any effect on the binding. On increasing the solvent polarity, the *cis*- to *trans*-conformer ratio of L-**1** increases from 0 in $CDCl_3$ to 1.10 in D_2O (Fig. S29a, ESI†), or from 0.45 in 7 : 3 (v/v) MeOH/PBS buffer through 1.05 in a 4 : 6 (v/v) mixture to 1.40 in a 2 : 8 (v/v) mixture (Table 2 and Fig. S30a, ESI†). Previously we showed that, in a 7 : 3 (v/v) mixture, L-**1** binds to L-/D-DOPA with a K_a^D/K_a^L value of 2.67 (Tables 1 and 2). We next examined the variations of absorption and CD spectra of L-**1** in mixtures of MeOH/0.05 M, pH 8.0 PBS buffer of higher water volume fractions, 4 : 6 and 2 : 8 (Fig. S31 and S32, ESI†). In the

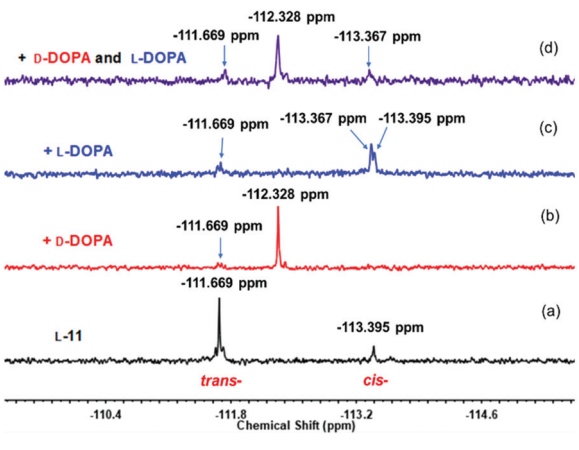

Fig. 5 ^{19}F NMR spectra of L-**11** (a) in the presence of D-DOPA (b) or L-DOPA (c) or a mixture of D-DOPA and L-DOPA (d) in 7 : 3 (v/v) MeOH/0.05 M, pH 8.0 PBS buffer (D_2O volume fraction 10%). [L-**11**] = 0.12 mM, [D-DOPA] = [L-DOPA] = 0.48 mM.

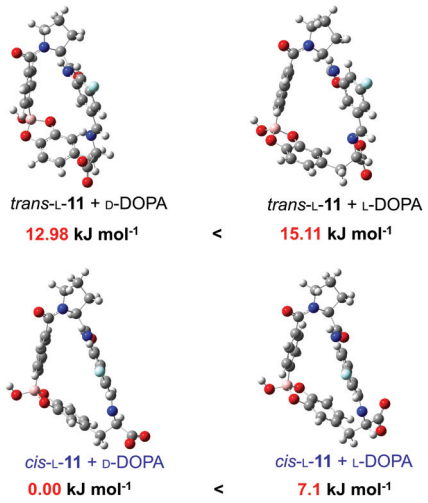

Fig. 6 DFT-optimized structures of *trans*-L-**11**/D-DOPA, *trans*-L-**11**/L-DOPA, *cis*-L-**11**/D-DOPA and *cis*-L-**11**/L-DOPA in H_2O at the B3LYP/6-31G* level (Fig. S28, ESI†). Energy data are relative.

Table 2 Binding constants (K_a) of receptors L-**1** and L-**5** with L-/D-DOPA in MeOH/buffer mixtures with varying compositions with D- to L-DOPA (K_a^D/K_a^L)[a]

			K_a/M^{-1}		
Receptor	MeOH/PBS (v/v)	Ratio (*cis*-/*trans*-)	L-DOPA	D-DOPA	K_a^D/K_a^L
L-**1**	7 : 3	0.45	$(6.44 \pm 0.99) \times 10^4$	$(1.72 \pm 0.18) \times 10^5$	2.67
	4 : 6	1.05	$(5.05 \pm 1.23) \times 10^4$	$(2.48 \pm 0.85) \times 10^5$	4.91
	2 : 8	1.40	—[b]	$(4.59 \pm 0.42) \times 10^4$	—
L-**5**	7 : 3	0.50	$(6.04 \pm 1.14) \times 10^4$	$(3.15 \pm 0.66) \times 10^4$	0.52
	4 : 6	0.88	$(2.44 \pm 0.83) \times 10^4$	$(3.15 \pm 1.32) \times 10^4$	1.29
	2 : 8	1.13	$(1.81 \pm 0.95) \times 10^3$	$(6.32 \pm 2.81) \times 10^4$	34.9

[a] Binding constants (K_a) were obtained by nonlinear fitting of the CD signal as a function of DOPA concentration assuming a 1 : 1 stoichiometry. [L-**1**] and [L-**5**] = 40 μM, T = 298 K. [b] Due to minor changes in CD spectra, accurate K_a values could not be fitted (for titration curves see Fig. S60–S66, ESI†).

4 : 6 (v/v) mixture in which the *cis*-conformer of L-**1** is more preferred, chiral recognition of D-/L-DOPA is enhanced with a K_a^D/K_a^L value of 4.91 (Table 2 and Fig. S31, ESI†), while in the 2 : 8 (v/v) mixture there is almost no response to L-DOPA (Fig. S32, ESI†). Similar spectral titrations were also performed with L-**5** by L- or D-DOPA in these three mixtures (Fig. S33 and S34, ESI†). The ratio K_a^D/K_a^L of L-**5** for D-/L-DOPA increases from 0.52 through 1.29 to 34.9 as the *cis*-L-**5** conformer is increasingly dominant upon increasing the polarity of the solution (Table 2 and Fig. S30b, ESI†). This change agrees with the DFT calculations that in DOPA-binding complexes the proline residue takes its *cis*-conformation. A change in the solvent composition of the MeOH/PBS-buffer mixture thus appears to be another approach for tuning the chiral recognition of proline-based receptors, despite the fact that the change of the reactivity to boronate and imine by solvent effects may also contribute.

Conclusions

In summary, we showed that with proline-based receptors bearing two different binding groups, the balancing of the two binding events does matter for the chiral recognition. Using boronic acid and aldehyde as the binding groups that are respectively attached *via* amide linkages into the N-/C- or C-/N-termini of the proline residue in the forms of phenylboronic acid and benzaldehyde, we found that, (i) the position of the boronic acid and aldehyde groups substituted on the two phenyl rings and (ii) the sites where phenylboronic acid and benzaldehyde are attached respectively at the N-/C- or C-/N-termini influence the chiral recognition of the created receptors towards L-/D-DOPA. A further increase in the binding ability of the weaker binding group, here the aldehyde group that interacts with the amine group in DOPA, by an electron-withdrawing fluorine atom substituted onto the benzaldehyde phenyl ring, thus better balancing the two binding events, results in an enhanced chiral recognition. Finally, we showed that on varying the solvent composition of the MeOH/PBS-buffer mixture to favour the *cis*-conformer of the proline residue in the case of L-**1**, chiral recognition of D-DOPA is enhanced. Controlling the conformation of the proline residue is therefore found to be another method for tuning the chiral recognition. The present choice of chiral recognition of DOPA that requires at least two different binding groups in the receptor molecule makes it possible to unveil these observations, good for extended exploration of proline based receptors for chiral recognition. These results are expected to be of significance in guiding the designing of receptors that rely on two or more binding events.

Experimental

Materials and methods

All reagents were purchased from commercial sources and were used without further purification. Flash chromatography was carried out on silica gel (300–400 mesh). ^{1}H NMR, ^{13}C NMR and ^{19}F NMR spectra ($CDCl_3$, CD_3OD or D_2O) were recorded on a Bruker AV500 MHz, AV600 MHz or AV850 MHz spectrometer. Mass spectra were acquired on a Bruker En Apex ultra 7.0 TFT-MS spectrometer. CD spectra were recorded on a Jasco J-810 spectropolarimeter. Absorption spectra were recorded on a Thermo Evolution 300 spectrometer with a 1 cm standard quartz cell. Job plots were obtained from CD measurements of 11 solutions of a fixed total concentration of L-**1** (or L-**11**) and D-DOPA at 40 μM. All calculations were carried out using Gaussian 16.

General procedures for the synthesis of proline derivatives

Compound a. Boc-L-proline (2.15 g, 10 mmol) was dissolved in dichloromethane under stirring in an ice bath, to which trimethylamine (2.5 mL) and isobutyl chloroformate (1.7 mL, 13 mmol) were added. The mixture was kept in the ice bath for 30 min, after which *m*-aminobenzaldehyde (1.82 g, 15 mmol) was added dropwise. The reaction mixture was stirred at room temperature and the progress of the reaction was monitored by TLC until completion. The solvent was removed under vacuum to lead to a solid product. This crude product was dissolved in ethyl acetate and washed with 0.1 M HCl (3 × 10 mL), a satu-

rated sodium bicarbonate solution (3 × 10 mL) and a saturated sodium chloride solution (3 × 10 mL), respectively, and the organic layer was dried with anhydrous $MgSO_4$. After evaporation of the solvent a crude oil was obtained and it was next subjected to chromatography on silica gel using petroleum ether/ethyl acetate (3 : 1, v/v) as the eluent to obtain a light yellow solid in 84% yield (2.67 g). Mp 182.5–184.5 °C. ^{1}H NMR (500 MHz, $CDCl_3$) δ (ppm) 9.95 (s, 1H), 9.82 (s, 1H), 8.06 (s, 1H), 7.72 (s, 1H), 7.56 (s, 1H), 7.44 (d, J = 30.6 Hz, 1H), 4.51 (s, 1H), 3.67–3.27 (m, 2H), 2.50 (s, 1H), 2.15–1.79 (m, 3H), 1.51 (s, 9H). ^{13}C{^{1}H} NMR (125 MHz, $CDCl_3$) δ (ppm) 192.1, 170.5, 156.7, 139.3, 137.1, 129.6, 125.3, 124.3, 121.0, 81.2, 60.5, 47.3, 28.4, 27.4, 24.6. HRMS (FTICR MS ESI$^+$) $[M + Na]^+$ calcd for $C_{17}H_{22}BKN_2O_4$: 357.1217, found 357.1217.

Compound c. Compound **a** (1.28 g, 4 mmol) was dissolved in 10 mL methylene dichloride, to which TFA (8 mL) was added dropwise and the mixture was stirred at room temperature for 2 h. The solvent was removed under reduced pressure to yield a light yellow oil **b**.

p-Bromobenzoic acid (1.24 g, 6 mmol) in dichloromethane (15 mL) was stirred at 0 °C, to which HOBt (1.05 g, 7.8 mmol), EDCI (1.72 g, 9 mmol), and trimethylamine (5 mL, 36 mmol) were added, and the resultant mixture was stirred at this temperature for 30 min. Then **b** dissolved in dichloromethane was added dropwise to the above mixture. The reaction was allowed to proceed under stirring at room temperature until completion as indicated by TLC. After evaporation, the crude product was diluted with ethyl acetate and the solution was washed with 0.1 M HCl (3 × 10 mL), aqueous $NaHCO_3$ (3 × 10 mL) and brine (3 × 10 mL), respectively. The organic layer was dried with anhydrous $MgSO_4$. After the solvent was evaporated, the crude product was chromatographed on silica gel using petroleum ether/ethyl acetate (3 : 1, v/v) as the eluent to afford a slightly yellow solid in 77.5% yield (1.86 g). Mp 180.2–181.5 °C. ^{1}H NMR (500 MHz, $CDCl_3$) δ (ppm) 9.92 (s, 1H), 9.77 (s, 1H), 8.08 (s, 1H), 7.71 (d, J = 6.0 Hz, 2H), 7.61 (d, J = 8.2 Hz, 1H), 7.55 (d, J = 7.4 Hz, 1H), 7.50 (d, J = 7.6 Hz, 1H), 7.39 (dd, J = 14.1, 6.3 Hz, 1H), 7.33 (t, J = 7.9 Hz, 1H), 4.97 (dd, J = 7.2, 4.9 Hz, 1H), 3.68–3.59 (m, 1H), 3.58–3.48 (m, 1H), 2.57 (dd, J = 11.2, 5.6 Hz, 1H), 2.23–2.10 (m, 2H), 1.94 (dt, J = 12.6, 6.9 Hz, 1H). ^{13}C NMR (125 MHz, $CDCl_3$) δ (ppm) 192.1, 170.0, 169.2, 139.2, 137.6, 137.0, 133.7, 130.2, 130.2, 129.5, 125.7, 125.3, 124.5, 122.7, 121.2, 61.0, 50.8, 27.2, 25.4. HRMS (FTICR MS ESI$^+$) $[M + Na]^+$ calcd for $C_{19}H_{17}BrNaN_2O_3$: 423.0320, found 423.0327.

Compound L-1. Compound **c** (0.69 g, 1.9 mmol), boronic acid pinacol ester (1.45 g, 5.7 mmol) and KOAc (1.14 g, 11.4 mmol) in DMF were stirred under nitrogen at room temperature for 30 min. Catalyst Pd(dppf)Cl_2 (0.19 g) was next added under a N_2 atmosphere. The reaction mixture was allowed to stir at 80 °C for 24 hours in an oil bath. Then, the mixture was cooled down and filtered. The filtrate was concentrated under reduced pressure to yield a crude solid product. The crude product was purified by silica gel chromatography eluted with petroleum ether/ethyl (10 : 1 to 4 : 1, v/v) as the eluent to afford solid L-**1** in 47% yield (0.40 g). Mp 196.0–197.7 °C. ^{1}H NMR (500 MHz, $CDCl_3$) δ (ppm) 9.89 (s, 1H), 9.81 (s, 1H), 8.06 (s, 1H), 7.80 (d, J = 7.8 Hz, 2H), 7.70 (d, J = 8.0 Hz, 1H), 7.53 (d, J = 7.3 Hz, 1H), 7.45 (d, J = 7.9 Hz, 2H), 7.37 (t, J = 7.8 Hz, 1H), 4.93 (dd, J = 7.5, 4.6 Hz, 1H), 3.46 (ddt, J = 24.0, 10.8, 6.6 Hz, 2H), 2.60 (dd, J = 11.5, 5.9 Hz, 1H), 2.02 (ddd, J = 19.9, 12.5, 6.8 Hz, 2H), 1.93–1.73 (m, 1H), 1.28 (s, 12H). ^{13}C{^{1}H} NMR (125 MHz, $CDCl_3$) δ (ppm) 192.1, 171.2, 169.9, 139.3, 138.2, 136.8, 134.9, 129.3, 126.3, 125.2, 123.9, 121.4, 84.2, 61.0, 50.7, 28.1, 25.4, 24.9, 24.61, 24.58. HRMS (FTICR MS ESI$^+$) $[M + Na]^+$ calcd for $C_{25}H_{29}BNaN_2O_5$: 471.2062, found 471.2073.

Compounds D-**1** to L-**10** and **12–14** were similarly synthesized following procedures given in Schemes S1–S14, ESI.†

Compound D-1. Light yellow solid, 0.38 g, 45% yield. Mp 196.4–197.3 °C. ^{1}H NMR (500 MHz, $CDCl_3$) δ (ppm) 9.97 (s, 1H), 9.87 (s, 1H), 8.14 (s, 1H), 7.87 (d, J = 7.8 Hz, 2H), 7.78 (d, J = 7.9 Hz, 1H), 7.60 (d, J = 7.5 Hz, 1H), 7.51 (d, J = 7.8 Hz, 2H), 7.44 (t, J = 7.8 Hz, 1H), 5.00 (dd, J = 7.6, 4.5 Hz, 1H), 3.65–3.35 (m, 2H), 2.78–2.55 (m, 1H), 2.07 (ddt, J = 18.8, 16.1, 7.7 Hz, 2H), 1.91 (dt, J = 12.5, 6.5 Hz, 1H), 1.35 (s, 12H). ^{13}C{^{1}H} NMR (125 MHz, $CDCl_3$) δ (ppm) 191.1, 172.0, 169.6, 136.9, 136.7, 133.1, 132.0, 131.0, 129.8, 128.0, 126.8, 119.5, 84.2, 61.1, 50.8, 27.1, 25.4, 24.9, 24.6, 24.3. HRMS (FTICR MS ESI$^+$) $[M + Na]^+$ calcd for $C_{25}H_{29}BNaN_2O_5$: 471.2062, found 471.2061.

Compound L-2. Light yellow solid, 0.35 g, 41% yield. Mp 235.7–237.5 °C. ^{1}H NMR (500 MHz, $CDCl_3$) δ (ppm) 10.09 (s, 1H), 9.93 (s, 1H), 7.89 (d, J = 8.1 Hz, 2H), 7.86 (d, J = 8.6 Hz, 2H), 7.76 (d, J = 8.6 Hz, 2H), 7.53 (d, J = 8.1 Hz, 2H), 5.03 (dd, J = 7.9, 4.3 Hz, 1H), 3.54 (dtd, J = 17.6, 10.8, 6.9 Hz, 2H), 2.80–2.64 (m, 1H), 2.19–2.00 (m, 2H), 1.93 (td, J = 13.2, 6.5 Hz, 1H), 1.38 (s, 12H). ^{13}C{^{1}H} NMR (125 MHz, $CDCl_3$) δ (ppm) 191.0, 171.7, 169.6, 143.9, 138.0, 134.9, 132.0, 130.9, 126.3, 119.5, 84.2, 61.1, 50.7, 27.2, 25.4, 24.9, 24.60, 24.58. HRMS (FTICR MS ESI$^+$) $[M + Na]^+$ calcd for $C_{25}H_{29}BNaN_2O_5$: 471.2062, found 471.2063.

Compound D-2. Light yellow solid, 0.45 g, 53% yield. Mp 244.5–246.0 °C. ^{1}H NMR (500 MHz, $CDCl_3$) δ (ppm) 10.08 (s, 1H), 9.89 (s, 1H), 7.87 (d, J = 7.7 Hz, 2H), 7.81 (d, J = 8.4 Hz, 2H), 7.72 (d, J = 8.4 Hz, 2H), 7.51 (d, J = 7.8 Hz, 2H), 5.00 (dd, J = 7.5, 4.6 Hz, 1H), 3.63–3.39 (m, 2H), 2.81–2.56 (m, 1H), 2.18–1.97 (m, 2H), 1.98–1.68 (m, 1H), 1.35 (s, 12H). ^{13}C{^{1}H} NMR (125 MHz, $CDCl_3$) δ (ppm) 191.1, 171.5, 169.9, 143.9, 138.1, 134.9, 131.9, 130.9, 126.2, 119.4, 84.2, 61.1, 50.7, 27.6, 25.4, 24.9, 24.66, 24.60. HRMS (FTICR MS ESI$^+$) $[M + Na]^+$ calcd for $C_{25}H_{29}BNaN_2O_5$: 471.2062, found 471.2069.

Compound L-3. Light yellow solid, 0.33 g, 39% yield. Mp 208.7–210.0 °C. ^{1}H NMR (500 MHz, $CDCl_3$) δ (ppm) 10.03 (s, 1H), 9.89 (s, 1H), 8.09 (s, 1H), 7.99 (s, 1H), 7.91 (d, J = 7.5 Hz, 1H), 7.73–7.67 (m, 1H), 7.66 (d, J = 7.7 Hz, 1H), 7.54–7.49 (m, 1H), 7.46 (t, J = 7.5 Hz, 1H), 7.35 (td, J = 7.8, 4.4 Hz, 1H), 5.10–4.94 (m, 1H), 3.61 (dtd, J = 16.9, 10.5, 6.7 Hz, 2H), 2.53 (dd, J = 13.3, 7.9 Hz, 1H), 2.29–2.07 (m, 1H), 1.89 (dd, J = 27.6, 21.5 Hz, 2H), 1.35 (s, 12H). ^{13}C{^{1}H} NMR (125 MHz, $CDCl_3$) δ (ppm) 192.2, 171.8, 169.6, 139.3, 136.8, 133.1, 129.8, 129.4, 128.0, 125.3, 124.0, 121.6, 84.2, 61.0, 50.8, 27.4, 25.4, 25.0,

24.9, 24.6. HRMS (FTICR MS ESI$^+$) [M + Na]$^+$ calcd for $C_{25}H_{29}BNaN_2O_5$: 471.2062, found 471.2068.

Compound L-4. Light yellow solid, 0.37 g, 43% yield. Mp 125.4–126.5 °C. ^{1}H NMR (500 MHz, $CDCl_3$) δ (ppm) 10.06 (s, 1H), 9.84 (s, 1H), 7.86 (s, 1H), 7.83 (d, J = 7.4 Hz, 1H), 7.76 (d, J = 8.4 Hz, 2H), 7.67 (d, J = 8.4 Hz, 2H), 7.54 (d, J = 7.7 Hz, 1H), 7.38 (t, J = 7.6 Hz, 1H), 4.94 (dd, J = 7.4, 4.5 Hz, 1H), 3.60–3.33 (m, 2H), 2.64 (dd, J = 11.9, 5.7 Hz, 1H), 2.12–1.91 (m, 2H), 1.87–1.74 (m, 1H), 1.27 (s, 12H). ^{13}C{^{1}H} NMR (125 MHz, $CDCl_3$) δ (ppm) 192.1, 171.8, 169.4, 139.2, 138.1, 137.0, 134.9, 129.5, 126.3, 125.5, 124.3, 121.5, 84.2, 61.0, 50.7, 27.1, 25.5, 24.9, 24.59, 24.58. HRMS (FTICR MS ESI$^+$) [M + Na]$^+$ calcd for $C_{25}H_{29}BNaN_2O_5$: 471.2062, found 471.2069.

Compound L-5. Light yellow solid, 0.31 g, 36% yield. Mp 114.0–116.1 °C. ^{1}H NMR (850 MHz, $CDCl_3$) δ (ppm) 10.08 (s, 1H), 9.26 (s, 1H), 7.98 (d, J = 6.4 Hz, 2H), 7.84 (d, J = 8.3 Hz, 2H), 7.72 (s, 2H), 7.54 (d, J = 5.5 Hz, 1H), 7.37–7.25 (m, 1H), 4.98 (s, 1H), 3.60 (s, 1H), 3.47 (s, 1H), 2.65 (s, 1H), 2.18 (s, 1H), 2.11 (s, 1H), 1.94 (s, 1H), 1.34 (s, 12H). ^{13}C {^{1}H} NMR (214 MHz, $CDCl_3$) δ (ppm) 191.5, 170.4, 168.5, 141.4, 137.6, 137.4, 130.6, 129.8, 128.5, 127.8, 127.8, 125.8, 122.8, 119.8, 118.2, 83.9, 60.9, 50.4, 26.9, 25.5, 24.9, 24.9. HRMS (FTICR MS ESI$^+$) [M + Na]$^+$ calcd for $C_{25}H_{29}BNaN_2O_5$: 471.2067, found 471.2063.

Compound L-6. Light yellow solid, 0.29 g, 34% yield. Mp 221.6–222.9 °C. ^{1}H NMR (850 MHz, $CDCl_3$) δ (ppm) 10.09 (s, 1H), 9.44 (s, 1H), 7.98 (d, J = 6.7 Hz, 2H), 7.78 (d, J = 7.2 Hz, 2H), 7.71 (d, J = 5.9 Hz, 2H), 7.60 (d, J = 6.7 Hz, 2H), 5.01 (s, 1H), 3.58 (s, 1H), 3.48 (s, 1H), 2.71 (s, 1H), 2.18 (s, 1H), 2.09 (s, 1H), 1.95 (s, 1H), 1.36 (s, 12H). ^{13}C{^{1}H} NMR (214 MHz, $CDCl_3$) δ (ppm) 191.4, 170.7, 168.3, 141.2, 140.7, 137.4, 135.8, 129.9, 129.0, 127.8, 118.8, 83.7, 61.1, 50.5, 26.4, 25.5, 24.88, 24.87. HRMS (FTICR MS ESI$^+$) [M + Na]$^+$ calcd for $C_{25}H_{29}BNaN_2O_5$: 471.2067, found 471.2063.

Compound L-7. Light yellow solid, 0.38 g, 45% yield. Mp 178.4–179.9 °C. ^{1}H NMR (850 MHz, $CDCl_3$) δ (ppm) 10.05 (s, 1H), 9.23 (s, 1H), 8.06 (s, 1H), 7.98 (d, J = 7.0 Hz, 1H), 7.84 (d, J = 7.4 Hz, 1H), 7.82 (s, 2H), 7.62 (t, J = 6.9 Hz, 1H), 7.52 (d, J = 6.0 Hz, 1H), 7.32 (t, J = 7.1 Hz, 1H), 4.96 (s, 1H), 3.62 (d, J = 7.2 Hz, 1H), 3.50 (d, J = 7.1 Hz, 1H), 2.64 (d, J = 5.6 Hz, 1H), 2.16 (d, J = 6.1 Hz, 1H), 2.09 (d, J = 6.4 Hz, 1H), 1.92 (d, J = 5.5 Hz, 1H), 1.32 (d, J = 9.2 Hz, 12H). ^{13}C{^{1}H} NMR (214 MHz, $CDCl_3$) δ (ppm) 191.3, 170.3, 168.5, 137.6, 136.9, 136.4, 133.0, 131.3, 130.6, 129.4, 128.5, 125.9, 122.9, 83.9, 61.0, 50.7, 30.2, 29.7, 26.8, 25.5, 24.88, 24.85. HRMS (FTICR MS ESI$^+$) [M + Na]$^+$ calcd for $C_{25}H_{29}BNaN_2O_5$: 471.2067, found 471.2062.

Compound L-8. White solid, 0.25 g, 29% yield. Mp 121.6–122.9 °C. ^{1}H NMR (850 MHz, $CDCl_3$) δ (ppm) 10.08 (s, 1H), 9.50 (s, 1H), 8.08 (s, 1H), 8.01 (s, 1H), 7.83 (s, 1H), 7.77 (d, J = 7.2 Hz, 1H), 7.66 (d, J = 7.2 Hz, 1H), 7.59 (d, J = 7.2 Hz, 1H), 7.47 (d, J = 7.2 Hz, 1H), 7.41 (d, J = 7.3 Hz, 1H), 5.00 (d, J = 18.4 Hz, 1H), 3.64 (s, 1H), 3.54 (s, 1H), 2.68 (s, 1H), 2.18 (s, 1H), 2.11 (s, 1H), 1.95 (s, 1H), 1.35 (s, 12H). ^{13}C{^{1}H} NMR (214 MHz, $CDCl_3$) δ (ppm) 191.2, 170.5, 168.5, 136.5, 135.8, 132.9, 131.9, 131.6, 129.5, 128.2, 121.4, 118.8, 116.7, 83.7, 61.1, 50.7, 26.6, 25.5, 24.88, 24.87. HRMS (FTICR MS ESI$^+$) [M + Na]$^+$ calcd for $C_{25}H_{29}BNaN_2O_5$: 471.2067, found 471.2074.

Compound L-9. White solid; 0.45 g, 57% yield. Mp 178.7–181.3 °C. ^{1}H NMR (500 MHz, $CDCl_3$) δ (ppm) 9.60 (s, 1H), 7.95 (s, 1H), 7.88 (d, J = 7.3 Hz, 1H), 7.61 (d, J = 7.4 Hz, 1H), 7.56 (d, J = 7.8 Hz, 2H), 7.43 (t, J = 7.4 Hz, 1H), 7.27 (dd, J = 9.4, 5.8 Hz, 2H), 7.05 (t, J = 7.2 Hz, 1H), 4.98 (s, 1H), 3.54 (dtd, J = 16.7, 10.3, 6.7 Hz, 2H), 2.64 (d, J = 4.7 Hz, 1H), 2.28–1.92 (m, 2H), 1.88 (dd, J = 12.0, 6.1 Hz, 1H), 1.34 (s, 12H). ^{13}C{^{1}H} NMR (125 MHz, $CDCl_3$) δ (ppm) 172.0, 168.8, 138.3, 136.7, 133.1, 129.8, 128.8, 127.9, 123.9, 119.8, 84.1, 60.8, 50.6, 26.6, 25.4, 24.9, 24.58, 24.56. HRMS (FTICR MS ESI$^+$) [M + Na]$^+$ calcd for $C_{24}H_{29}BNaN_2O_4$: 443.2113, found 443.2116.

Compound L-10. Light yellow solid, 0.26 g, 80% yield. Mp 120.8–122.5 °C. ^{1}H NMR (500 MHz, $CDCl_3$) δ (ppm) 9.92 (s, 1H), 9.77 (s, 1H), 8.08 (s, 1H), 7.71 (d, J = 6.0 Hz, 2H), 7.61 (t, J = 9.1 Hz, 1H), 7.55 (d, J = 7.4 Hz, 1H), 7.50 (d, J = 7.6 Hz, 1H), 7.39 (dd, J = 14.1, 6.3 Hz, 1H), 7.33 (t, J = 7.9 Hz, 1H), 4.97 (dd, J = 7.2, 4.9 Hz, 1H), 3.68–3.60 (m, 1H), 3.58–3.50 (m, 1H), 2.57 (dd, J = 11.2, 5.6 Hz, 1H), 2.22–2.10 (m, 2H), 1.96–1.92 (dt, J = 12.6, 6.9 Hz, 1H). ^{13}C{^{1}H} NMR (125 MHz, $CDCl_3$) δ (ppm) 192.1, 170.0, 169.2, 139.1, 137.6, 137.0, 133.7, 130.2, 129.5, 125.7, 125.3, 124.5, 122.7, 121.2, 61.0, 50.8, 27.2, 25.4. HRMS (FTICR MS ESI$^+$) [M + Na]$^+$ calcd for $C_{19}H_{17}BrNaN_2O_3$: 425.0294, found 425.0294.

Compound L-11. Light yellow solid, 0.35 g, 38% yield. Mp 198.0–199.0 °C. ^{1}H NMR (500 MHz, $CDCl_3$) δ (ppm) 10.15 (s, 1H), 9.88 (s, 1H), 7.91 (d, J = 7.5 Hz, 2H), 7.76 (s, 1H), 7.72 (d, J = 10.1 Hz, 1H), 7.56 (d, J = 7.7 Hz, 2H), 7.25 (d, J = 7.6 Hz, 1H), 5.04–4.92 (m, 1H), 3.73–3.58 (m, 1H), 3.54 (dd, J = 15.0, 8.2 Hz, 1H), 2.66–2.46 (m, 1H), 2.21–2.07 (m, 2H), 1.94 (dd, J = 13.6, 7.7 Hz, 1H), 1.38 (s, 12H). ^{13}C NMR (125 MHz, $CDCl_3$) δ (ppm) 190.7, 169.9, 163.6, 140.8, 138.2, 138.0, 134.9, 126.2, 117.6, 112.4, 109.5, 84.2, 61.0, 50.7, 29.1, 27.8, 25.4, 24.9. HRMS (FTICR MS ESI$^+$) [M + Na]$^+$ calcd for $C_{25}H_{28}BFNaN_2O_5$: 489.1973, found 489.1968.

Compound L-12. Light yellow solid, 0.32 g, 34% yield. Mp 106.5–107.8 °C. ^{1}H NMR (500 MHz, $CDCl_3$) δ (ppm) 9.98 (s, 1H), 9.71 (s, 1H), 8.14 (s, 1H), 7.78 (d, J = 7.9 Hz, 1H), 7.68 (d, J = 7.5 Hz, 1H), 7.62 (d, J = 7.6 Hz, 1H), 7.59 (d, J = 9.8 Hz, 1H), 7.45 (dd, J = 15.0, 7.5 Hz, 2H), 5.01 (dd, J = 7.3, 3.0 Hz, 1H), 3.50 (dt, J = 11.5, 5.6 Hz, 1H), 3.41 (dd, J = 17.8, 7.4 Hz, 1H), 2.63 (dd, J = 10.4, 5.4 Hz, 1H), 2.17–2.08 (m, 2H), 2.05–1.91 (m, 1H), 1.37 (s, 12H). ^{13}C{^{1}H} NMR (125 MHz, $CDCl_3$) δ (ppm) 192.1, 169.0, 167.5, 139.0, 137.0, 130.9, 129.6, 127.9, 125.5, 124.5, 121.9, 121.4, 84.5, 60.8, 49.0, 29.7, 27.2, 24.9, 24.6. HRMS (FTICR MS ESI$^+$) [M + Na]$^+$ calcd for $C_{25}H_{28}BFNaN_2O_5$: 489.1973, found 489.1988.

Compound L-13. Light yellow solid, 0.19 g, 20% yield. Mp 182.5–184.0 °C. ^{1}H NMR (500 MHz, $CDCl_3$) δ (ppm) 9.93 (s, 1H), 9.71 (s, 1H), 8.11 (s, 1H), 7.78 (s, 1H), 7.66 (d, J = 7.4 Hz, 1H), 7.57 (d, J = 9.7 Hz, 1H), 7.43 (dd, J = 13.6, 6.8 Hz, 1H), 4.99 (s, 1H), 3.48 (dd, J = 13.5, 6.7 Hz, 1H), 3.46–3.31 (m, 1H), 2.57 (s, 1H), 2.11 (m, 2H), 1.94 (m, 1H), 1.34 (s, J = 9.7 Hz, 12H). ^{13}C NMR (214 MHz, $CDCl_3$) δ (ppm) 192.1, 172.1, 169.1, 139.2, 138.1, 137.1, 134.9, 129.6, 126.2, 125.5, 124.4, 121.5,

84.2, 60.8, 50.6, 29.7, 26.6, 25.4, 24.9, 24.6. HRMS (FTICR MS ESI$^+$) $[M - H]^-$ calcd for $C_{25}H_{26}BF_2N_2O_5$: 483.1903, found 483.1900.

Compound L-14. Light yellow solid, 0.28 g, 30% yield. Mp 164.7–166.1 °C. ^{1}H NMR (850 MHz, $CDCl_3$) δ (ppm) δ 10.38 (s, 1H), 9.09 (s, 1H), 7.93 (t, J = 7.3 Hz, 1H), 7.82 (d, J = 8.1 Hz, 1H), 7.79 (s, 1H), 7.52 (d, J = 7.2 Hz, 1H), 7.42 (d, J = 7.9 Hz, 1H), 7.37 (d, J = 9.9 Hz, 1H), 7.31 (t, J = 7.7 Hz, 1H), 4.89 (dd, J = 7.6, 4.3 Hz, 1H), 3.58 (dt, J = 10.4, 6.9 Hz, 1H), 3.45 (dt, J = 10.4, 6.9 Hz, 1H), 2.59 (dd, J = 11.4, 5.4 Hz, 1H), 2.17 (dd, J = 13.1, 6.6 Hz, 1H), 2.08 (dt, J = 20.6, 7.6 Hz, 1H), 1.95–1.85 (m, 1H), 1.32 (s, 12H). ^{13}C NMR (125 MHz, $CDCl_3$) δ (ppm) 186.4, 167.8, 164.8, 163.6, 147.1, 143.4, 137.5, 130.9, 130.7, 129.2, 128.9, 128.5, 124.5, 124.0, 123.3, 122.9, 115.8, 115.7, 83.9, 65.6, 61.0, 50.4, 31.5, 29.7, 24.9. HRMS (FTICR MS ESI$^+$) $[M + Na]^+$ calcd for $C_{25}H_{28}BFNaN_2O_5$: 489.1973, found 489.1991.

Conflicts of interest

There are no conflicts to declare.

Acknowledgements

We are grateful to the NSF of China (Grants 21435003, 91427304, 21521004, 91856118 and 21820102006) and to the Ministry of Education (MOE) of China Program for Changjiang Scholars and Innovative Research Team in University (Grant IRT13036) for support.

Notes and references

1 (*a*) M. G. Bomar, B. Song, P. Kibler, K. Kodukula and A. K. Galande, *Org. Lett.*, 2011, **13**, 5878–5881; (*b*) M.-K. Chung, P. S. White, S. J. Lee, M. R. Gagné and M. L. Waters, *J. Am. Chem. Soc.*, 2016, **138**, 13344–13352; (*c*) A. J. Metrano, N. C. Abascal, B. Q. Mercado, E. K. Paulson, A. E. Hurtley and S. J. Miller, *J. Am. Chem. Soc.*, 2017, **139**, 492–516.

2 E. Lenci and A. Trabocchi, *Chem. Soc. Rev.*, 2020, DOI: 10.1039/d0cs00102c.

3 A. Moyano and R. Rios, *Chem. Rev.*, 2011, **111**, 4703–4832.

4 L.-E. Guo, Y. Hong, S.-Y. Zhang, M. Zhang, X.-S. Yan, J.-L. Cao, Z. Li, T. D. James and Y.-B. Jiang, *J. Org. Chem.*, 2018, **83**, 15128–15135.

5 (*a*) W. Poewe, A. Antonini, J. C. M. Zijlmans, P. R. Burkhard and F. Vingerhoets, *Clin. Interv. Aging*, 2010, **5**, 229–238; (*b*) T. Alexander, C. E. Sortwell, C. D. Sladek, R. H. Roth and K. Steece-Collier, *Cell Transplant.*, 1997, **6**, 309–315.

6 (*a*) G. Grigorean and C. B. Lebrilla, *Anal. Chem.*, 2001, **73**, 1684–1691; (*b*) B. Polak, W. Gołkiewicz and T. Tuzimski, *Chromatographia*, 2006, **63**, 197–201; (*c*) B. Yuan, H. Wu, T. Sanders, C. Mccullum, Y. Zheng, P. B. Tchounwou and Y. M. Liu, *Anal. Biochem.*, 2011, **416**, 191–195; (*d*) T. Hasegawa, K. Takahashi, T. Fukiwake, M. Saijo and Y. Motoki, *Food Hyg. Saf. Sci.*, 2013, **54**, 379–383; (*e*) Y. J. Kang, J. W. Oh, Y. R. Kim, J. S. Kim and H. Kim, *Chem. Commun.*, 2010, **46**, 5665–5667.

7 (*a*) T. Pradhan, H. S. Jung, J. H. Jang, T. W. Kim, C. Kang and J. S. Kim, *Chem. Soc. Rev.*, 2014, **43**, 4684–4713; (*b*) J.-L. Chen, X.-P. Yan, K. Meng and S.-F. Wang, *Anal. Chem.*, 2011, **83**, 8787–8793; (*c*) F. M. Raymo and M. A. Cejas, *Org. Lett.*, 2002, **4**, 3183–3185; (*d*) D. Guo, P. Ran, C. Chen, Y. Chen, C. Xuan and Y. Fu, *J. Electrochem. Soc.*, 2015, **162**, 354–359; (*e*) S. Ates, E. Zor, I. Akin, H. Bingol, S. Alpaydin and E. G. Akgemci, *Anal. Chim. Acta*, 2017, **970**, 30–37.

8 (*a*) K. E. Secor and T. E. Glass, *Org. Lett.*, 2004, **6**, 3727–3730; (*b*) A. Chaicham, S. Sahasithiwat, T. Tuntulani and T. Boosayarat, *Chem. Commun.*, 2013, **49**, 9287–9289; (*c*) X.-X. Chen, X. Wu, P. Zhang, M. Zhang, B.-N. Song, Y.-J. Huang, Z. Li and Y.-B. Jiang, *Chem. Commun.*, 2015, **51**, 13630–13633.

9 (*a*) B. T. Herrera, S. L. Pilicer, E. V. Anslyn, L. A. Joyce and C. Wolf, *J. Am. Chem. Soc.*, 2018, **140**, 10385–10401; (*b*) H. H. Jo, C.-Y. Lin and E. V. Anslyn, *Acc. Chem. Res.*, 2014, **47**, 2212–2221.

10 (*a*) C. Grathwohl and K. Wüthrich, *Biopolymers*, 1976, **15**, 2025–2041; (*b*) R. W. Newberry, B. VanVeller, I. A. Guzei and R. T. Raines, *J. Am. Chem. Soc.*, 2013, **135**, 7843–7846; (*c*) M. Kuemin, Y. A. Nagel, S. Schweizer, F. W. Monnard, C. Ochsenfeld and H. Wennemers, *Angew. Chem., Int. Ed.*, 2010, **49**, 6324–6327.

11 C. Godoy-Alcántar, A. K. Yatsimirsky and J. M. Lehn, *J. Phys. Org. Chem.*, 2005, **18**, 979–985.

12 (*a*) I. Tirotta, V. Dichiarante, C. Pigliacelli, G. Cavallo, G. Terraneo, F. B. Bombelli, P. Metrangolo and G. Resnati, *Chem. Rev.*, 2015, **115**, 1106–1129; (*b*) R. E. London and S. A. Gabel, *J. Am. Chem. Soc.*, 1994, **116**, 2562–2569; (*c*) J. Axthelm, S. H. C. Askes, M. Elstner, U. Reddy G, H. Görls, P. Bellstedt and A. Schiller, *J. Am. Chem. Soc.*, 2017, **139**, 11413–11420.

13 (*a*) H. Gan, A. G. Oliver and B. D. Smith, *Chem. Commun.*, 2013, **49**, 5070–5072; (*b*) Y. Zhao and T. M. Swager, *J. Am. Chem. Soc.*, 2013, **135**, 18770–18773; (*c*) X. Wu, X.-X. Chen and Y.-B. Jiang, *Analyst*, 2017, **142**, 1403–1414.

14 C. Siebler, B. Maryasin, M. Kuemin, R. S. Erdmann, C. Rigling, C. Grunenfelder, C. Ochsenfeld and H. Wennemers, *Chem. Sci.*, 2015, **6**, 6725–6730.

